

**INVESTIGATION OF LUMINESCENCE STUDIES ON  $\text{Tm}^{3+}$  DOPED KBr  
SINGLECRYSTALS**S. Bangaru<sup>1\*</sup>, V. Shanmugam<sup>2</sup><sup>1\*</sup>Associate professor of Physics, Arignar Anna Government Arts College,  
Namakkal-637002, India.<sup>2</sup>Ph.D Scholar in Physics, Arignar Anna Government Arts College,  
Namakkal-637002, India.

---

**ABSTRACT:-**  $\text{Tm}^{3+}$  doped KBr single crystals have been grown from melted by using a Bridgemanstockbarger technique. The characterizations are Optical absorption-transmittance, Photoluminescence [PL], Thermo luminescence [TL], Powder X-Ray diffraction [PXRD], Laser Raman spectroscopy and Scanning Electron Microscopy [SEM]. The optical absorption - transmittance study confirms the suitability of the grown crystals for optical device applications. UV- Vis transmittance spectrum was recorded in the range 190-1100nm. PL emission wavelength was observed around at 451nm blue emission with 350nm excitation. This 451nm attributed to the  $^1G_4 \rightarrow ^3H_6$  transition. The grown crystals have been subjected to PXRD studies to determine the lattice parameters have been calculated and are presented. It is observed that crystallizes is in Hexagonal system with space group  $Fm\bar{3}m$ . SEM micrograph analysis, the particle size ranges from few microns to 5 $\mu\text{m}$ . Trap parameters for the TL glow curve were calculated by Chen's peak shape method. TL emission confirms the participation of Thulium ions in the recombination process in host material.

---

**Keywords:** Optical absorption, PL, TL, Laser Raman, PXRD, SEM

**1. INTRODUCTION**

Luminescence properties of trivalent rare earth ion ( $\text{Tm}^{3+}$ ) is doped with the alkali halide (KBr) and due to their optical applications such as optical storage systems, color displays and medical have been earlier reported work on many researchers[1,2].  $\text{Tm}^{3+}$  ions has twelve electrons filled in the 4f shell ( $4f^{12}$ ) and it is very useful for the electron transition process[3]. The most commonly used access in Rare Earth( $\text{Tm}^{3+}$ ) is doped light emitting diodes (LEDs) is the blue light luminescence, accommodate a broadband emission in the visible region for PL process[4,5]. Blue (or) other colored light can also be obtained via PL process in lanthanide doped materials[6,7], and exhibits great applications in color displays, high density optical data storage and reading, optical communications and biomedical diagnostics[8-13], etc. Their capacity incorporates high concentrations of rare earth (RE) ions and also makes them suitable candidates for expansion of activate photonic devices[14]. However, the choice of the host material is extremely important for the advance of efficient PL due to Optical devices based on RE doped crystals. In the emission spectra of the rare earth ions the different host materials, an important role belongs to the electron interaction, which determines the redistribution of PL process. As well as the  $\text{Tm}^{3+}$  doped KBr single crystals is famous dosimetric material used for measurement of ionizing radiation. Thulium ions have several advantages which have high absorption cross section and broad band absorption in the 190-1100nm spectral range. The blue emission band of trivalent thulium( $\text{Tm}^{3+}$ ) ions wavelength located around at 451nm as reported in earlier work[15]. Alkali halides due to their understandable structure have made the discerning of many properties of insulators possible, particularly with regard to calculation of defect parameters and ionic conduction etc. Alkali halides have a broad range of lattice parameters, which makes it possible to absorb impurity ions of different sizes and valence states in the lattices[16-19]. In the present work, namely  $\text{Tm}^{3+}$  doped KBr single crystals were grown by Bridgeman Stockbarger technique. The grown crystals were characterized by Optical absorption, Photoluminescence [PL], Thermoluminescence [TL], Laser Raman spectroscopy, Scanning Electron Microscope (SEM), Powder X-Ray diffraction(PXRD).

## 2. EXPERIMENTAL DETAIL

Single crystals of pure KBr (99.99% purity) and thulium doped KBr (99.99% purity) were grown using the Bridgman Stockbarger technique. Thulium was added in the form of thulium fluoride (Aldrich 99.99% purity).

The crystals were grown in three different concentrations of the impurity 1%, 3% and 5% by weight. Samples of size approximately  $5 \times 5 \times 1 \text{ mm}^3$  were used for all except the PL studies. For PL  $5 \times 5 \times 3 \text{ mm}^3$  samples were used. The results of the three concentrations were similar and hence only the results pertaining to a thulium concentration of 3% by weight are presented and discussed. The absorption and transmittance spectra were recorded using a Perkin Elmer Lambda 35UV-Vis spectrophotometer in the region 190–1100nm. PL spectra were recorded at room temperature using Perkin Elmer LS 55 Luminescence spectrometer in the region 200–900 nm with a spectral width of 5 nm. TL emission was recorded using a Perkin Elmer LS 55 with the excitation slit being closed. The phase of the PXRD crystals was confirmed by X-Ray diffractometer using  $\text{CuK}\alpha$  radiation. The microstructure of the grown crystals was studied using Scanning Electron Microscopy SEM-JEOL-JSM-5610LV model. The Laser Raman Spectroscopy were recorded at ReinsaawInvia spectrometer model ( $\lambda_L=700\text{nm}$ ). Before TL experiment the crystals were annealed at  $400^\circ\text{C}$  for half an hour and then quenched to room temperature to ensure homogeneous distribution of impurity and to remove any storage effect.

## 3. OPTICAL ABSORPTION

The optical absorption spectra of  $\text{Tm}^{3+}$  doped KBr single crystals is as shown in Fig.1. curve (a), the 260 and 329nm absorption band is due to the exciton absorption of the host matrix [20]. The sharp absorption peaks are 357nm, 463nm, 688nm, 696nm, 696nm, 774nm and 793nm which are attributed to the transitions of  $^3\text{H}_6 \rightarrow ^1\text{D}_2$ ,  $^3\text{H}_6 \rightarrow ^1\text{G}_4$ ,  $^3\text{H}_6 \rightarrow ^3\text{F}_2$ ,  $^3\text{H}_6 \rightarrow ^1\text{D}_2$  and  $^3\text{H}_6 \rightarrow ^3\text{F}_3$  respectively with in  $4f^{12}$  electronic configuration of  $\text{Tm}^{3+}$  ions [21].

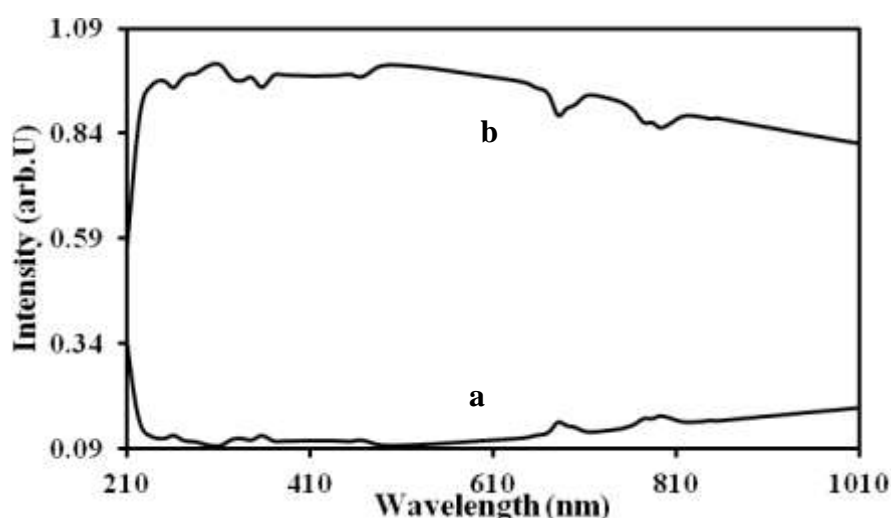


**Fig.1 Curve(a) Optical Absorption , Curve (b) Transmittance Spectrum of  $\text{Tm}^{3+}$  doped KBr Single Crystals**

This absorption lines are depended weakly on the host, since the 4f electrons are effectively shield by the filled SS and SP orbitals of  $\text{Tm}^{3+}$  ions. The optical transmittance of KBr:  $\text{Tm}^{3+}$  single crystals is shown in Fig1 Curve (b). It was recorded in the region 190- 1100nm using LAMBDA-35 UV-Vis spectrometer, which includes near UV, visible and far IR regions. This transmittance wavelengths are matched the absorption wavelengths, so the result was the grown crystal that is fully transparent and it is very useful for optical device applications.

## 4. PHOTOLUMINESCENCE

The photoluminescence is the most direct way to make light from a solid material. Rare earth based luminescent materials have considerable particle applications in almost optical device involving the artificial production of light[22-24].

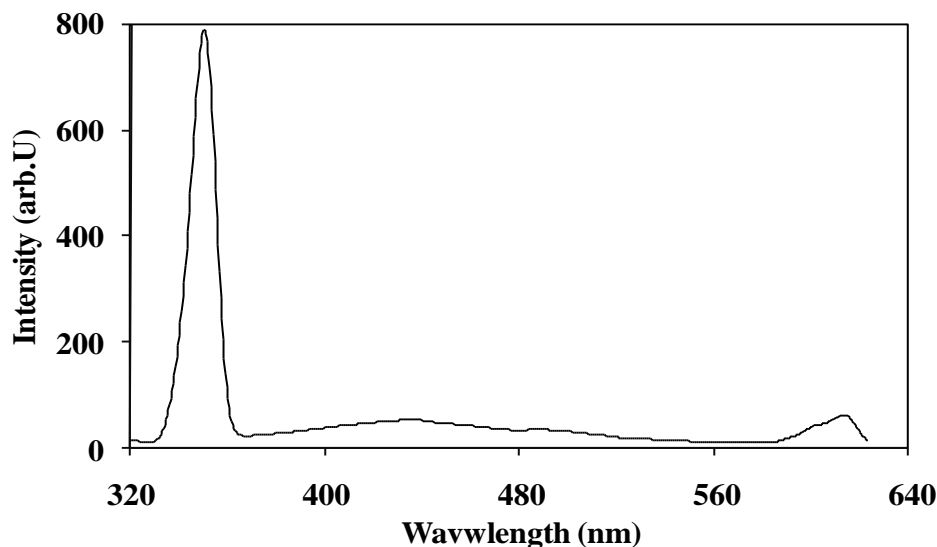


**Fig.2 Excitation spectrum of KBr:Tm<sup>3+</sup> Emission at 450nm**

Fig.2 shows the PL excitation spectrum of 1m doped KBr crystals with emission wavelength at 450nm. The excitation band wavelength consists of one sharp peak centered at 351nm which is in the visible region and assigned due to the intraconfigurational 4f shell transitions from the ground to excited state levels of Tm<sup>3+</sup> ion. Weak band centered at 444 and 618nm. Recently studies on KYbNW<sub>4</sub>O<sub>2</sub> : Tm<sup>3+</sup> have identified the rare Tm<sup>3+</sup> ion related 4f-4f transition [25], Tm<sup>3+</sup> with 4f<sup>12</sup> electronic configuration has complicated energy levels, so it is excitation spectrum containing of broad peaks due to 4f-4f transition of Tm<sup>3+</sup> ions.

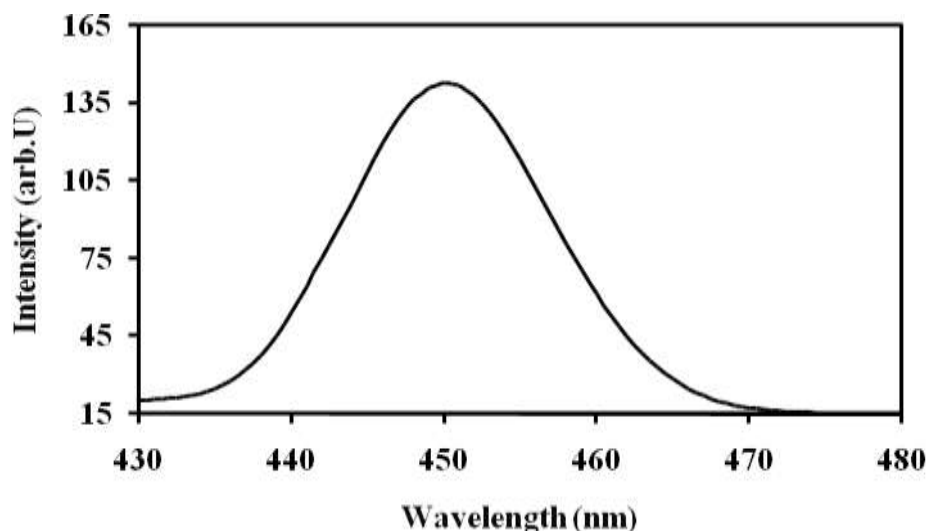


**Fig.3 Emission Spectrum of KBr:Tm<sup>3+</sup> for excitation at 350 nm**

Fig.3. shows the PL emission spectrum of Tm<sup>3+</sup> doped KBr single crystals with excitation wavelength at 350nm and exists the single broad emission band centered at 451nm, in the blue region. The Tm<sup>3+</sup> ion in G emits a 451nm photon and returns to the H, through the <sup>1</sup>G<sub>4</sub>→<sup>3</sup>H<sub>6</sub> transition [26]. In general, Tm<sup>3+</sup> ion have complicated energy level schemes, due to the strong deviation from the 4f electronic configuration, and thus, through many paths, the relaxation of the excited states of Tm<sup>3+</sup> ions can take place, giving rise to Ultraviolet, Visible, and Infrared emission with moderate intensity [27-29]. Among these emissions, in this case the Ultraviolet emission possesses the stronger intensity with high color purity, which may be used as blue light emitting process. Therefore, KBr:Tm<sup>3+</sup> was prepared and investigated. In this investigation indicates the KBr host doped Tm<sup>3+</sup> ions were exists an excellent luminescent property for optical device applications.

## 5. THERMOLUMINESCENCE GLOW CURVE

The TL glowcurve of  $\text{KBr:Tm}^{3+}$  crystals is shown in Fig.4. The grown crystal before taking TL were annealed at  $400^\circ\text{C}$  and then irradiated at a  $\gamma$ -ray dose of 5GY. TL was taken out soon after the irradiation to ignore the circumstance of error.

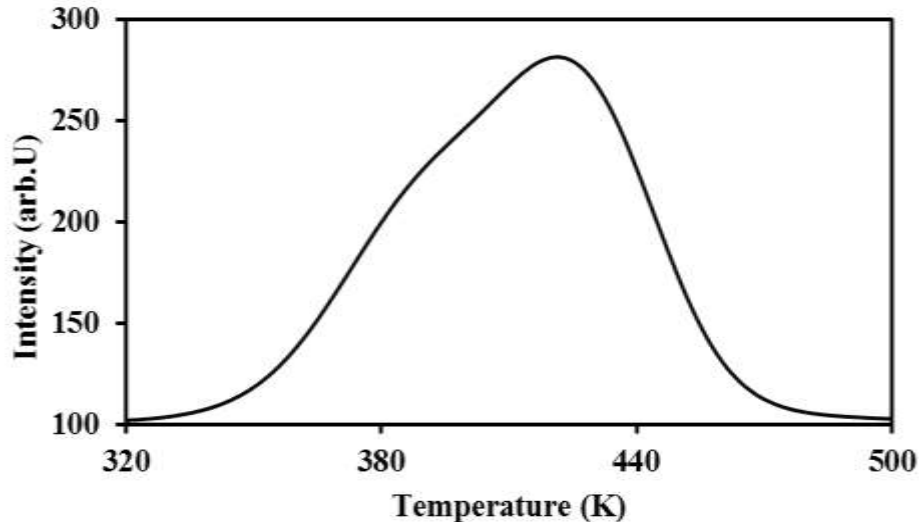


**Fig.4 Thermoluminescence Spectrum of  $\text{KBr:Tm}^{3+}$  Crystals after  $\gamma$ - ray irradiation for 1-hour**

The TL was observed up to 600K at a heating rate of  $120^\circ\text{C}/\text{min}$ . the glow curve reveals one clear and well distinguished peak at 422K. The TL intensity of this sample is low compared with the standard thermoluminescence dosimetry (TLD) material and therefore does not have any specific application in dosimetry. The TL glow curve are very useful to analyze the nature of traps present in the material and also gives us information about the energy absorbed by the material during irradiation. The kinetic parameters such as activation energy (E) and frequency factor(s) gives information about defect centers cause TL in the material [30]. So, we calculated these parameters of the prepared sample. The dosimetry properties of the TL materials mainly depend on the kinetic parameters of the glow peak. Considering this aspect, the parameters were calculated using Chen's peak shape method. This method is one of the broadly used technique to determine the kinetic parameters of the glow peak of TL materials.

For the calculation of these parameters the following shape parameters were to be evaluated  $\omega = T_2 - T_1$  (total half intensity width),  $\delta = T_2 - T_m$  (high temperature half width) and  $\tau = T_m - T_1$  (low temperature half width). The order of kinetics can be evaluated from the geometric factor ( $\mu_g$ ) of the glow peak ( $\mu = \delta/\omega$ ) and depends on the glow peak. The value of  $\mu_g$  for second order kinetics is 0.48. The geometric factor is around below 0.5 and indicates that the crystal obeys second-order kinetics. The activation energy (E) and frequency factor(s) can be calculated from equations as was reported in earlier work [31]. The trap depth for 422K glow peak is 0.88eV, frequency factor for 422K glow peak were found to be  $1.32 \times 10^9 \text{ s}^{-1}$ . From the data, the peak at low temperature (i.e) 422K is due to low energy traps. From this, we conclude that low temperature peak are related with shallow traps.

## 6. THERMOLUMINESCENCE EMISSION

TL emission of  $\text{KBr:Tm}^{3+}$  consist of two distinguishable emission peak at 440nm is Fig.5 (curve a) and 475nm is Fig.5 (curve b) corresponds to glow peak temperature at 422K. Among both emission band, the peak with high intensity peak 475K is overtake for deconvolution. The deconvolution formed by means of using software "Origin 5.0". TL deconvoluted emission were carried out on  $\text{KBr:Tm}^{3+}$  single crystals between the wavelength 300-700nm. The deconvoluted TL emission spectrum consists of two well distinguished peaks at 442nm and 503nm as shown in Fig.6. The PL emission band wavelength observed at 451nm assigned to the ( $^1\text{G}_4 \rightarrow ^3\text{H}_6$ ) transition of  $\text{Tm}^{3+}$  ions [26].

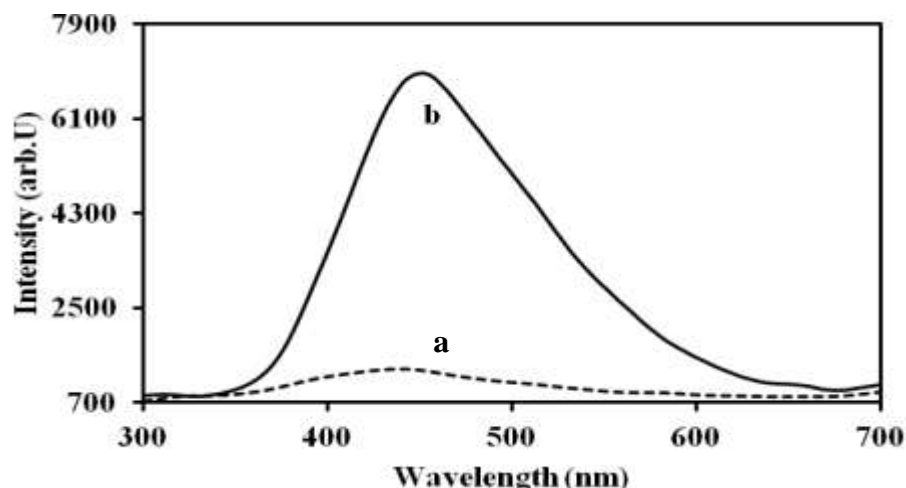


Fig.5 TL Emission spectrum of  $\text{KBr:Tm}^{3+}$  at (a) 440 K , (b) 475 K

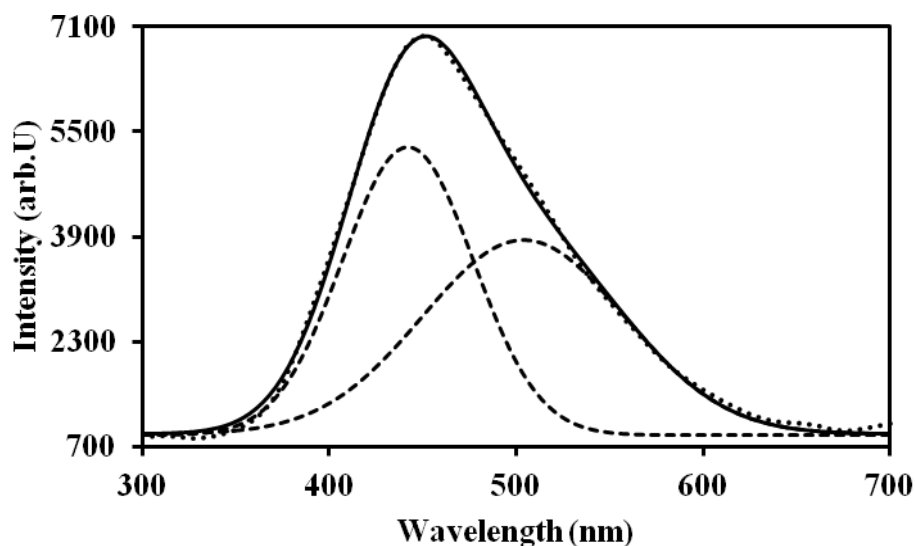


Fig.6 TL Emission Spectrum of  $\text{KBr:Tm}^{3+}$  Crystals for glow peak at 475 K

The TL and PL emission peaks more or less equal wavelength 444nm and 451 nm respectively. So this confirms that emission is only due to  $\text{Tm}^{3+}$  ions and involves the recombination of  $\text{Tm}^{3+}$  electrons. TL emission process is due to thermal release of  $\text{Tm}^{3+}$  electrons and their consequent recombination with hole centers. The comparison of PL and TL emission bands are shown in table.1

Table.1 Comparison of wavelength in Optical absorption, Photoluminescence and Deconvoluted TL emission of  $\text{KBr:Tm}^{3+}$  single crystals

Optical absorption		Photoluminescence		Thermoluminescence
Name	Absorption Wavelength (nm)	Excitation bands Wavelength (nm)	Emission bands Wavelength (nm)	Deconvoluted emission band in nm. Temperature at 475K
$\text{KBr : Tm}^{3+}$	357 ( $^3\text{H}_6 \rightarrow ^1\text{D}_2$ )	351	451 ( $^1\text{G}_4 \rightarrow ^3\text{H}_6$ )	442
	463 ( $^3\text{H}_6 \rightarrow ^1\text{G}_4$ )	444		503
	688 ( $^3\text{H}_6 \rightarrow ^3\text{F}_2$ )	618		
	774 ( $^3\text{H}_6 \rightarrow ^1\text{D}_2$ )			
	793 ( $^3\text{H}_6 \rightarrow ^3\text{F}_3$ )			

## 7. SCANNING ELECTRON MICROSCOPY

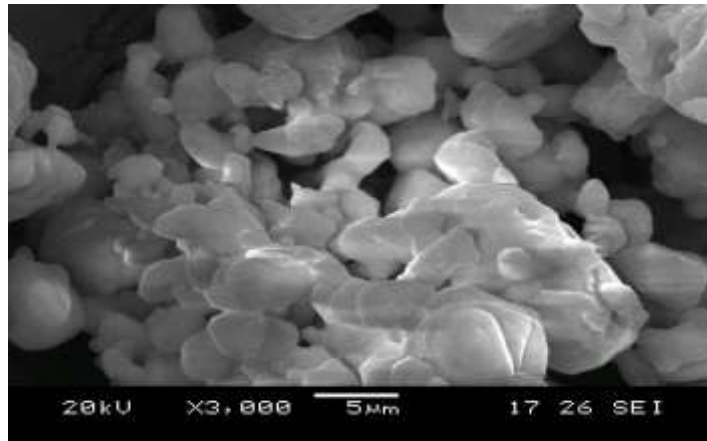


**Fig.7 SEM image of  $\text{KBr:Tm}^{3+}$  Single crystals**

The SEM micrograph of the  $\text{Tm}^{3+}$  doped KBr single crystals as shown in Fig.7. The grown crystals were subjected to x1000 magnification and accelerating voltage value of 20KV. The surface observed like a flower structure with agglomeration. The particle size is approximately few microns to  $5\mu\text{m}$  for the grown crystals. The SEM micrograph of the grown crystals which find that the particles are irregular in shapes. So we can terminate the SEM results in good agreement with the result obtained from XRD results.

## 8. LASER RAMAN SPECTROSCOPY

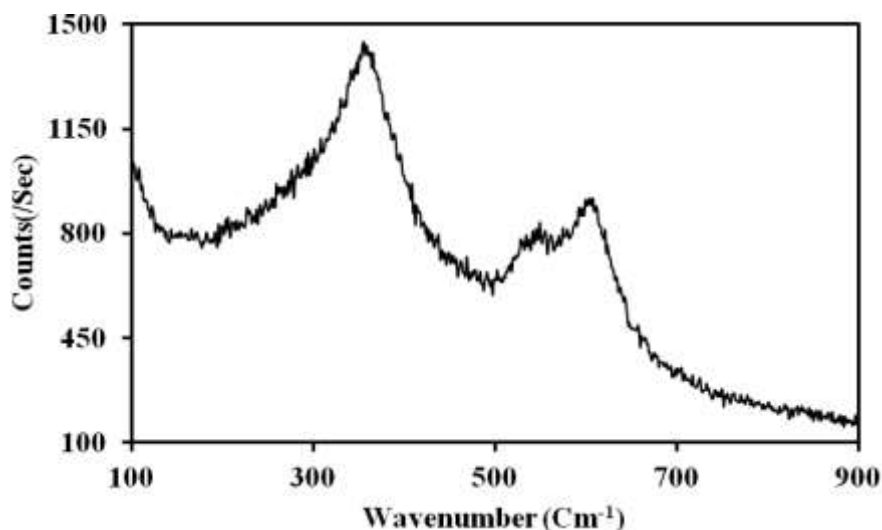


**Fig.8 Laser Raman scattering spectrum of  $\text{KBr:Tm}^{3+}$  crystals**

The Raman spectrum have using red laser excitation. The wavelength observed at room temperature as shown in Fig.8 for the  $\text{Tm}^{3+}$  doped KBr crystals. It composed of three main peaks of  $355\text{cm}^{-1}$ ,  $549\text{cm}^{-1}$  and  $607\text{cm}^{-1}$ . The earlier work reported as Raman modes have been observed frequencies around at  $141\text{cm}^{-1}$  for  $\text{Br}_3^-$  (stretching vibration) and  $216\text{cm}^{-1}$  for  $\text{Br}_2^-$  type[32]. The excitation band wavelength observed around at  $549\text{cm}^{-1}$  assigned to the first overtone of  $355\text{cm}^{-1}$  mode. The lattice modes of the crystalline bromide observed at  $549\text{cm}^{-1}$  and  $607\text{cm}^{-1}$  superposed to the second order spectrum of the host. The second order scattering bands have been reported by other authors at  $983\text{cm}^{-1}$ ,  $1030\text{cm}^{-1}$  and  $1160\text{cm}^{-1}$ [33]. In the present work the band observed at  $355\text{cm}^{-1}$ ,  $549\text{cm}^{-1}$  and  $607\text{cm}^{-1}$  are assigned to second order scattering.



## 9. POWDER X-RAY DIFFRACTION SPECTRUM

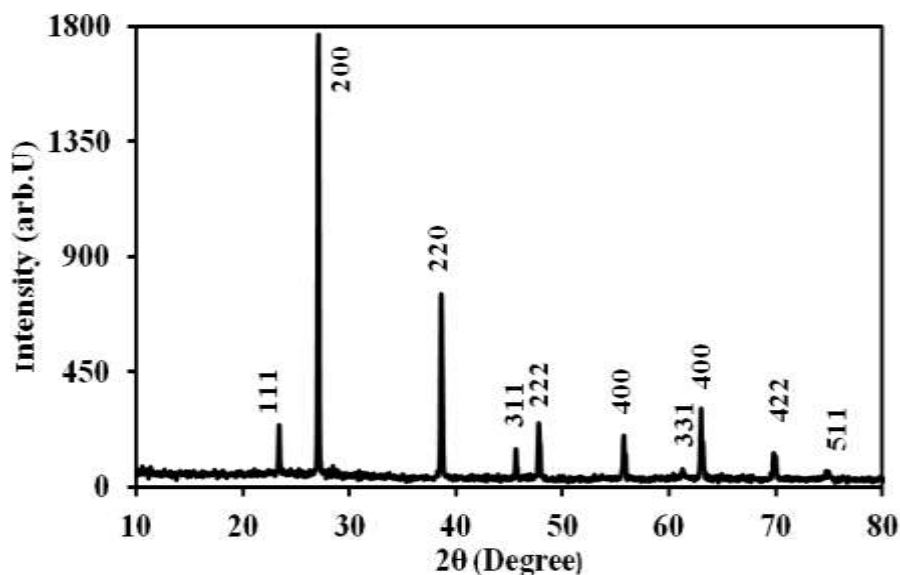


**Fig.9 PXRD pattern of the  $\text{KBr:Tm}^{3+}$  Crystals**

Fig.9 shows the powder x-ray diffraction pattern of the  $\text{Tm}^{3+}$  doped KBr single crystals used the  $\text{CuK}\alpha$  radiation ( $1.5406\text{\AA}$ ). Hence the powder x-ray diffraction pattern of the grown crystals were used to calculate the crystalline structure and crystallite size. The grown crystals are good and well crystalline nature with the high intensity peak  $2\theta = 27^\circ$  corresponding to the hkl diffraction plane [200]. This crystals have observed that the all diffractionspeaks compared with the standard data of pure KBr (JCPDS Card No:04-0531)[34]. It exhibits seven different peaks at  $2\theta$  values are  $23.3^\circ$ ,  $27^\circ$ ,  $38.5^\circ$ ,  $45.6^\circ$ ,  $47.7^\circ$ ,  $55.7^\circ$ ,  $61.2^\circ$ ,  $62.9^\circ$ ,  $69.9^\circ$  and  $75^\circ$  corresponding to diffraction planes are (1,1,1), (2,0,0), (2,2,0), (3,1,1), (2,2,2), (4,0,0), (3,3,1), (4,0,0), (4,2,2) and (5,1,1) respectively. The lattice parameters are  $a=b=7.95\text{\AA}$ ,  $c=8.84\text{\AA}$  and  $\alpha=\beta=\gamma=90^\circ$ . It is observed crystalline structure in hexagonal system of pure KBr with the space group  $\text{Fm}\bar{3}\text{m}$ . KBr can be observed indicating the dopant is well incorporated into the host lattice. So the grown sample obtained in a single phase and that doping with the small amount of  $\text{Tm}^{3+}$  will not induce any impurity phase. The average crystallite size of the grown crystal is  $8.5\mu\text{m}$ . It was calculated by Scherrer's formula  $D=k\lambda/\beta\cos\theta$ , Where  $k$  is the dimensionless shape factor indicate that the value of about 0.9,  $\lambda$  is the X-ray diffraction wavelength ( $\lambda=1.5406\text{\AA}$ ),  $\theta$  is the diffraction angle of high intensity peak and  $\beta$  is the full width half maximum of high intensity peak[35].

## CONCLUSION

The present paper  $\text{KBr:Tm}^{3+}$  is a good material for optical display devices. Optical absorption study reveals the transparency of the grown crystals. PL broad blue emission wavelength observed at  $451\text{nm}$  in  $\text{KBr:Tm}^{3+}$  crystals, which is due to ( $^1\text{G}_4 \rightarrow ^3\text{H}_6$ ) transition of  $\text{Tm}^{3+}$  ion. The results of a TL glow curve pattern of the grown crystals shows one prominent peak  $422\text{K}$ . Furthermore, the kinetic parameters, i.e., activation energy ( $E$ ), frequency factor(s) have been calculated. The TL emission peak confirms  $\text{Tm}^{3+}$  ion and it is involved in blue light emitting process. From the PXRD analysis, the calculated average crystallite size is  $8.5\mu\text{m}$ . The laser Raman scattering observed at  $355\text{cm}^{-1}$ ,  $549\text{cm}^{-1}$  and  $607\text{cm}^{-1}$  are assigned to second order scattering. SEM reveals that the microcrystalline morphology of the  $\text{Tm}^{3+}$  doped KBr single crystals is like a flower shape of particles and are various size from few microns to  $5\mu\text{m}$ .

## Acknowledgement

The authors great fully acknowledges UGC (RGNF) for providing financial support and UGC – DAE Consortium for scientific Research, IGCAR, Kalpakkam, India for providing experimental support.

## References

- [1]. M.A.Dugay, J.A.Giordmaine, P.M.Rentzepis, Display system using two-photon fluorescent materials, U.S.Patent, vol.3, pp.541-542 (1970).
- [2]. J.L.Cantatore, D.A.kriegel, Laser surgery: An approach to the pediatric patient, J Am Acad Dermatol, vol.50, pp.165-184 (2004).
- [3]. A.S.S.de Camargo, M.R.B. Andreetta, A.C. Hernandes, L.A.O. Nunes, 1.8  $\mu\text{m}$  emission and excited state absorption in LHPG grown  $\text{Gd}_{0.8}\text{La}_{0.2}\text{VO}_4:\text{Tm}^{3+}$  single crystal fibers for miniature lasers, Opt. Mater., vol. 28, pp.551-555 (2006).
- [4]. E.F.Schubert, light-emitting diodes, Cambridge university press. Cambridge. 2006.
- [5]. F.K.Yam, Z.Hassam, Innovative advances in LED technology, Microelectron. J., vol. 36, pp.129-137 (2005).
- [6]. F.E.Auzel, "Materials and devices using double-pumped phosphors with energy transfer," Proc.IEEE, vol. 61, pp.758-786 (1973) .
- [7]. Y.Ledemi, D.Manzani, S.J.L.Ribeiro, Y.Messasseq, Multicolor up conversion emission and color tenability in  $\text{Yb}^{3+}/\text{Tm}^{3+}/\text{Ho}^{3+}$  triply doped heavy metal oxide glasses, Opt. Mater., vol.33, pp. 1916-1920 (2011).
- [8]. S.Q.Xu, Z.M.Yang, J.J.Zhang, G.N.Wang, S.X.Dai, L.L.Hu, Z.H.Jiang, Upconversion fluorescence spectroscopy of  $\text{Er}^{3+}$ ,  $\text{Yb}^{3+}$  codoped leghemoglobin oxy fluoro silicate glass, Chem, Phys, Lett, vol. 385, pp.263-267 (2004).
- [9]. G.S.Qin, W.P.Qin, C.F.Wu, S.H.Huang, J.S.Zhang, S.Z.Lu, D.Zhano, H.Q.Liu, Enhancement of ultraviolet upconversion in  $\text{Yb}^{3+}$  and  $\text{Tm}^{3+}$  codoped amorphous fluoride film prepared by pulsed laser deposition, J. Appl. Phys., vol. 93, pp.4328-4330 (2003).
- [10]. V.karunakaran, J.Luis Perez Lustres, L.Zhao, N.P.Ernsting, O.S.etiz, Large dynamic stokes shift of DNA intercalation dye thiazole orange has contribution from a high-frequency mode, J Am Chem Soc, vol. 128, pp.2954-2962 (2006).
- [11]. V.A.G.Rivera, L.C.Barbosa, Spectroscopic properties of  $\text{Er}^{3+}$  doped sodium modified tellurite glass for uses optical amplifiers at 1540nm, J. Lumin, vol. 156, pp.116-123 (2014).
- [12]. V.A.G.Rivera, Y.Ledmi, M.El-Amraoui, Y.Messaddeq, E.Marega Jr. control of the radiative properties via Photon-Plasmon interaction in  $\text{Er}^{3+}$ ,  $\text{Tm}^{3+}$  codoped tellurite glass in the near infrared region, Opt. Exp., vol. 22, pp.21122-21136 (2014).
- [13]. M.Pollnau, D.R.Gamelin, S.R.Luthi, H.U.Gudel, M.P.Hehlen, Power dependence of upconversion luminescence in lanthanide and transition-metal-ion systems, Phys. Rev.B, vol. 61, 3337-3346 (2000).
- [14]. J.E.C.Silva, G.F.de sa, P.A.Santa-cruz, White light simulation by up-conversion in fluoride glass host, J. Alloys. Comp., vol.334, pp.260-263 (2002).
- [15]. G.M. Cai, N. Yang, H.X. Liu, J.Y. Si, Y.Q. Zhang, Single-phased and color tunable  $\text{LiSrBO}_3:\text{Dy}^{3+}$ ,  $\text{Tm}^{3+}$ ,  $\text{Eu}^{3+}$  phosphors for white-light-emitting application, J. Lumin., vol. 187, pp.211-220 (2017).
- [16]. V.Ausin, J.L.Alvarez Rivas, Thermoluminescence and F-Centers thermal annealing in heavily irradiated KCl and NaCl crystals, J. Phys C: Solid State Phys., vol. 7, 2255-2262 (1974).
- [17]. A.A.Braner, M.Iraeli, Effect of Illumination on the Thermoluminescence of Alkali halides, Phys. Rev., vol. 132, pp.2501-2505 (1963).
- [18]. B.Chandra, A.R.Lakshmanan, R.C.Bhatt, Effect of Deep Traps on the Sensitation in LiF (TLD-100) Phosphor, Phys. Status Solidi A, vol.60, pp.593-598 (1980).
- [19]. G.T.Hageseth, Optical Absorption and Thermoluminescence of X-Ray Irradiated KBr Crystals at Room Temperature, Phys. Rev. B, vol.5, pp.4060-4064 (1972).
- [20]. P.Christoberselvan, S.Selvasekarapandian, Optical Absorption, Photoluminescence and Thermally Stimulated Luminescence of  $\text{CsCl}:\text{Tb}$  Crystals, Phys. Status Solidi. B, vol. 194, pp.747-756 (1996).
- [21]. R.Reisfeld, Y.Eckstein, Absorption and emission spectra of thulium and erbium in borate and phosphate glasses, J. solid state chem., vol. 5, pp.174-185 (1972).
- [22]. K.Park and M.H.Heo, VUV Photoluminescence of  $(\text{Gd}, \text{Zn})\text{PO}_4:\text{Tb}^{3+}$  Phosphors Synthesized by Ultrasonic Spray Pyrolysis, Met. Mater. Int., vol. 17, pp.1027-1030 (2011).
- [23]. Abdul Kareem Parchur, Raghumani Singh Ningthoujam, Shyam Bahadur Rai, Gunadhor Singh Okram, Ram Asaray Singh, Mohit Tyagi, S.C.Gadkari, Raghendra Tewari and Rajesh Kumar Vatsa, Luminescence properties of  $\text{Eu}^{3+}$  doped  $\text{CaMoO}_4$  nanoparticles, Dalton Trans, vol.40, pp.7595-7601 (2011).
- [24]. M.S.Kwon, H.L.Park, T.W.Kim, Y.Huh, W.Choi and J.Y.Lee, Sol-gel Synthesis and Luminescence Property of Nanocrystalline  $\text{Y}_2\text{O}_3:\text{Eu}$  Phosphor using Metal Nitrate Precursors, Met. Mater. Int., vol. 12, pp.263-267 (2011).



- [25]. M.C.Pujol, F.Guell, X.Mateos, Jna.Gavalda, R.Sole, J.Massons, M.Aguilo, F.Diaz, Crystal growth and spectroscopic characterization of  $\text{Tm}^{3+}$  doped  $\text{KYbNbO}_4\text{O}_2$  single crystals, *Phys.Rev.B*, vol. 66, pp.144304-1 – 144304-8 (2002) .
- [26]. V.A.G.Rivera, F.A.Ferri, L.A.O.Nunes, E.Marega Jr., Whight light generation via up-conversion and blue tone in  $\text{Er}^{3+}/\text{Tm}^{3+}/\text{Yb}^{3+}$  doped zinc-tellurite glasses, *Opt. Mater.*, vol.67, pp.25-31 (2017).
- [27]. L.Wu, Y.Zhang, M.Gui, P.Lu, L.Zhao, S.Tian, Y.Kong and J.Xu, Luminescence and energy transfer of a color tunable phosphor:  $\text{Dy}^{3+}$ ,  $\text{Tm}^{3+}$ , and  $\text{Eu}^{3+}$  coactivated  $\text{KSr}_4(\text{BO}_3)_3$  for warm white UV LEDs, *J. Mater. Chem.*, vol. 22, pp.6463-6470 (2012).
- [28]. Z.J.Zhang, J.L.Yuan, X.J.Wang, D.B.Xiong, H.H.Chen, J.T.Zhao, Y.B.Fu, Z.M.Qi, G.B.Zhang, C.S.Shi, Luminescence properties of  $\text{CaZr}(\text{PO}_4)_2\text{:RE}$  ( $\text{RE} = \text{Eu}^{3+}$ ,  $\text{Tb}^{3+}$ ,  $\text{Tm}^{3+}$ ) under x-ray and VUV–UV excitation, *J.Phy. D: Appl.Phy.*, vol. 40, pp.1910-1914 (2007).
- [29]. T.Grzyb, A.Szczeszak, J.Rozowska, J.Legendziewicz and S.Lis, Tunable Luminescence of  $\text{Sr}_2\text{CeO}_4\text{:M}^{2+}$  ( $\text{M} = \text{Ca, Mg, Ba, Zn}$ ) and  $\text{Sr}_2\text{CeO}_4\text{:Ln}^{3+}$  ( $\text{Ln} = \text{Eu, Dy, Tm}$ ) Nanophosphors, *J. Phys. Chem. C*, vol. 116, pp.3219-3226 (2012).
- [30]. D.JosephDainel, U.Madhusoodanan, R.Nithya, P.Ramasamy, Irradiation, effect on luminescence properties of fluoroperovskite single crystal ( $\text{LiBaF}_3\text{:Eu}^{2+}$ ), *Radiat. Phys. Chem.*, vol.96, pp.135-139 (2014).
- [31]. A.H.Oza, N.S.Dhoble, K.Park, S.J.Dhoble, Synthesis and thermoluminescence characterizations of  $\text{Sr}_2\text{B}_5\text{O}_9\text{Cl:Dy}^{3+}$  phosphor for TL dosimetry, *J.Lumin.*, (2014).
- [32]. A.G.Maki, R.Forneris, Infrared and raman spectra of some trihalides ions  $\text{ICl}_2$ ,  $\text{IBr}_2$ ,  $\text{I}_3$ ,  $\text{I}_2\text{Br}$  and  $\text{BrICl}$ , *Spectrochim. Acta*, vol.23, pp.867-880 (1967).
- [33]. S.Dogra, J.Singh, N.D.Sharma, K.Samanta, H.K.Poswal, S.M.Sharma, A.K.Bandyopadhyay, Phase progression via phonon modes in lanthanide dioxides under pressure, *Vib. Spectrosc.*, vol. 70, pp.193-199 (2014).
- [34]. Swanson, Tatge, Calcium Fluoride,  $\text{CaF}_2$ , *Nat 'l. Bur. Stand. (US) Circ*, vol. 539, pp. 1-66 (1951).
- [35]. Sh.Dorendrajitsingh, S.Nambram, S.D.Meetei, Synthesis And Photoluminescence Study Of  $\text{Gd}_2\text{O}_3\text{:Dy}^{3+}$  Nanophosphors For White Light Applications, *Int.J.Lumin.Appli.*, vol.5, pp.380-383 (2015).